Detecting weak physical signals from noise: A machine-learning approach with applications to magnetic navigation

Sponsored by AFOSR

Ying-Cheng Lai
Arizona State University
4/24/2023

Collaborators:

Zheng-Meng Zhai, Mohammadamin Moradi, Ling-Wei Kong (ASU PhD students)
Dr. Aaron Nielsen, Air Force Institute of Technology

Magnetic Navigation - An Alternative to GPS Navigation

Dr. Aaron Canciani, AFIT

Dr. John Raquet, AFIT

- Robust aerial navigation without GPS is challenging;
- Alternative navigation systems for airborne use are often limited by where and when they can operate (e.g., terrain following systems cannot operate over oceans; star-tracker and computer-vision systems depend on weather and daylight)
- The Earth's magnetic anomaly field is globally available at all times, which has the potential to overcome many of the limitations and can be exploited for non-GPS based aerial navigation.

NAVIGATION
JOURNAL OF THE INSTITUTE OF NAVIGATION
ION

Original Article | Full Access

Absolute Positioning Using the Earth's Magnetic Anomaly Field†

Correction(s) for this article

Aaron Canciani, John Raquet

First published: 21 June 2016 | https://doi.org/10.1002/navi.138 | Citations: 32

Airborne Magnetic Anomaly Navigation

January 2017 · IEEE Transactions on Aerospace and Electronic Systems

DOI: 10.1109/TAES.2017.2649238

Aaron Canciani · John Raquet

Earth's Magnetic Field

Generated from inside the earth:

- Core field - 20-60 mT: dominant, responsible for the working of compasses
- **Anomaly field** - about 100 nT: due to the permanent or induced magnetization of the rocks in the earth's crust

Key feature of the anomaly field:

- **The strength of the anomaly field depends on the location – possible for positioning and navigation**
- **When collected from, e.g., an airplane, the anomaly field is effectively a time series signal**

Generated outside of the earth:

- Temporally varying field - about 10 nT: from the ionosphere, magnetosphere, and the coupling currents between the two

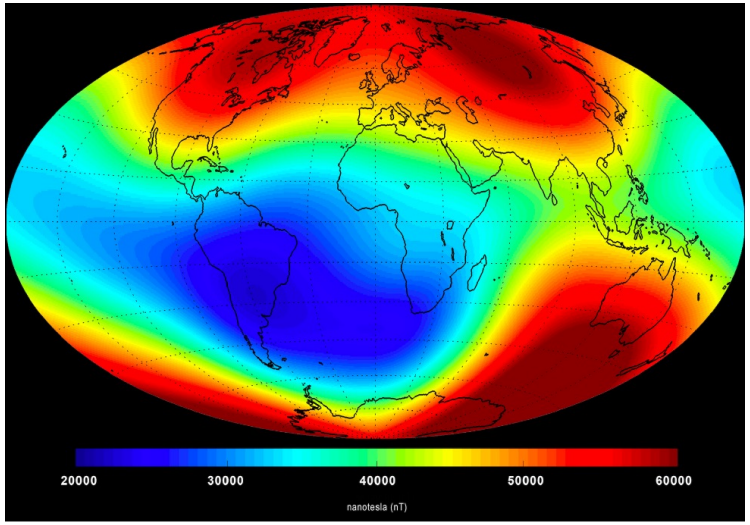

NASA Earth Observatory, "Measuring Earth's Magnetism," 2014. https://earthobservatory.nasa.gov/images/84266/measuring-earths-magnetism

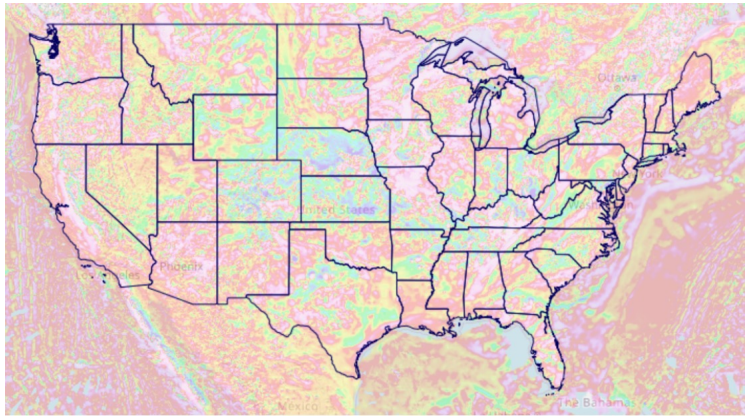

U.S. Geological Survey, "Magnetic anomaly maps and data for North America," 2021. https://mrdata.usgs.gov/magnetic/

How to Obtain the Earth Magnetic Field $\vec{B}_e$ from Aircraft Measurements?

Total measured field: $\vec{B}_m = \vec{B}_e + \vec{B}_{aircraft} = \vec{B}_{core} + \vec{B}_{anomaly} + \vec{B}_{tv} + \vec{B}_{aircraft}$

- $\vec{B}_{core}$ - calculated from the International Geomagnetic Reference Field (IGRF) coefficients
- $\vec{B}_{tv}$ - mostly from the diurnal variations and space weather – can be removed using ground-based reference measurements
- $\vec{B}_{aircraft}$- total field generated by the aircraft

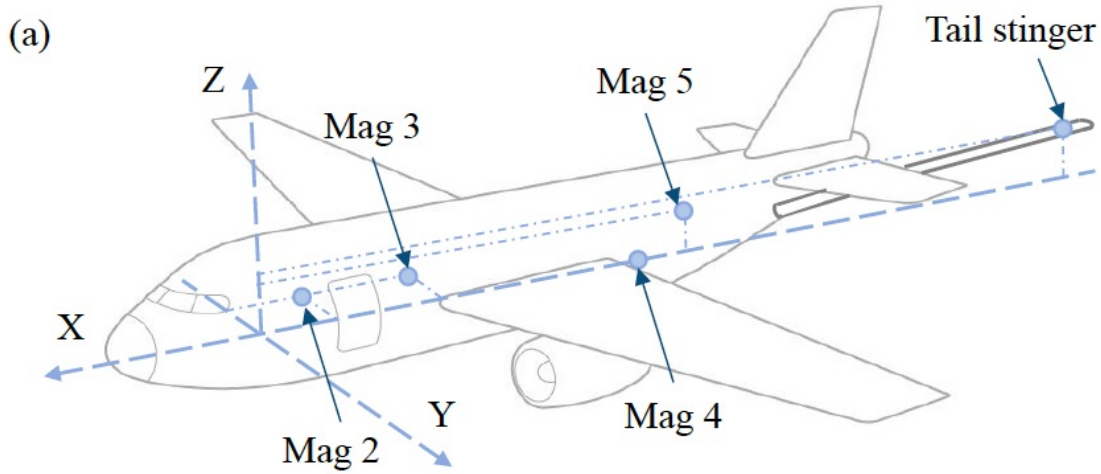

- **Calibration: Tolles-Lawson (TL) model** to estimate $\vec{B}_{aircraft}$
- Applied to the reading of the magnetometer at the tail stinger → real value of the earth field $\vec{B}_e$
- Subtracting $\vec{B}_{core}$ and $\vec{B}_{tv}$ from $\vec{B}_e$ gives the anomaly field $\vec{B}_{anomaly}$

Tolles-Lawson Model

TL model: the magnetic field generated by the body of the aircraft as three magnetic moments:

1. Permanent magnetic moment: the nearly constant magnetic moment of the entire aircraft.
2. Induced magnetic moment: the magnetic response of the magnetically susceptible materials in the aircraft to the earth magnetic field.
3. Eddy current moment: caused by the temporal variations of the earth magnetic field due to the motion of the aircraft.

$$
\begin{aligned}
B_{\mathrm{TL}} &= B_{\mathrm{perm}} + B_{\mathrm{ind}} + B_{\mathrm{eddy}} \\
&= \vec{B}_{\mathrm{m}}^{T} \begin{bmatrix} x_1 \\ x_2 \\ x_3 \end{bmatrix} + |\vec{B}_{\mathrm{m}}| \vec{B}_{\mathrm{m}}^{T} \begin{bmatrix} x_4 & x_5 & x_6 \\ x_5 & x_7 & x_8 \\ x_6 & x_8 & x_9 \end{bmatrix} \vec{B}_{\mathrm{m}} \\
&\quad + |\vec{B}_{\mathrm{m}}| \vec{B}_{\mathrm{m}}^{T} \begin{bmatrix} x_{10} & x_{11} & x_{12} \\ x_{13} & x_{14} & x_{15} \\ x_{16} & x_{17} & x_{18} \end{bmatrix} \dot{\vec{B}}_{\mathrm{m}},
\end{aligned}
$$

$$
|\vec{B}_{\mathrm{e,\ TL}}| = |\vec{B}_{\mathrm{m}}| - B_{\mathrm{TL}}
$$

- $x_1, \cdots, x_{18}$: 18 constant coefficients that can be calculated after a calibration flight
- TL model works well only when the flying aircraft is in a magnetically quiet mode and all the magnetometer measurements are performed on a tail stinger outside the cabin

- **Often this is not the case!**

Estimate of Earth's Anomaly Magnetic Field

- Recall:

$$\vec{B}_e = \vec{B}_{core} + \vec{B}_{anomaly} + \vec{B}_{tv}$$

- TL calibration gives an estimate of $\vec{B}_e$:

$$\hat{\vec{B}}_e = \vec{B}_{e,TL}$$

- $\vec{B}_{core}$ - calculated with the International Geomagnetic Reference Field (IGRF) coefficients
- $\vec{B}_{tv}$ - mostly from the diurnal variations and space weather – can be removed using ground-based reference measurement

$$\rightarrow \vec{B}_{anomaly} \approx \vec{B}_{e,TL} - \vec{B}_{core} - \vec{B}_{tv}$$

- *TL calibration works well only when the flying aircraft is in a magnetically quiet mode and all the magnetometer measurements are performed on a tail stinger outside the cabin.*
- *For normal flights, these conditions are not met.*
- ***Magnetic signals collected inside the cockpit are noisy due to the electronics – a weak signal embedded in overwhelmingly strong noise!***
- Use TL model to obtain the ground truth for training neural networks

Data Source: USAF-MIT Artificial Intelligence Accelerator

README.md

Signal Enhancement for Magnetic Navigation Challenge Problem

gitlab

This is a repository for the signal enhancement for magnetic navigation (MagNav) challenge problem, which was introduced at JuliaCon 2020. The high-level goal is to use magnetometer (magnetic field) readings recorded from within a cockpit and remove the aircraft magnetic noise to yield a clean magnetic signal. A detailed description of the challenge problem can be found here and additional MagNav literature can be found here.

Round	Start	End	Winning Team
1	26-Jul-20	28-Aug-20	Ling-Wei Kong, Cheng-Zhen Wang, and Ying-Cheng Lai Arizona State University (submission)
2	24-Sep-20	31-Jan-21	

Introduction Videos

- Magnetic Navigation Overview
- Challenge Problem Description
- Challenge Problem Datasets

Starter Code

A basic set of starter Julia code files have been provided within the `src` folder. This code is largely based on work done by Major Canciani. This code has only been tested with Julia 1.4 and 1.5. A sample run file is located within the `runs` folder, which includes downloading the flight data via artifact (`Artifacts.toml`). Details of the flight data are described in the readme files within the `readmes` folder. The flight data can also be directly downloaded from here.

Team Members

The MagNav team is part of the USAF-MIT Artificial Intelligence Accelerator, a joint collaboration between the United States Air Force, MIT CSAIL, and MIT Lincoln Laboratory. Current team members include:

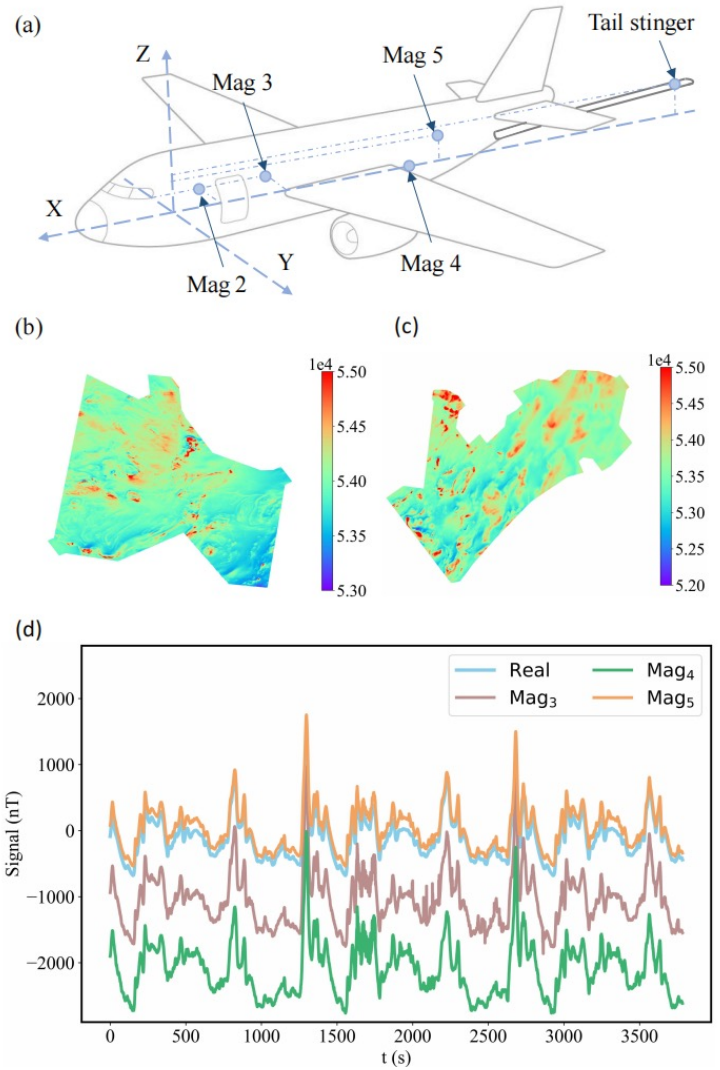

Data Structure

- Source: Open Call for developing machine-learning approaches to signal enhancement for magnetic navigation (MagNav) Challenge organized in 2020 by the Air Force-MIT Artificial Intelligence Accelerator
- Four other magnetometers placed at different positions in the cabin
- 45 available flight lines

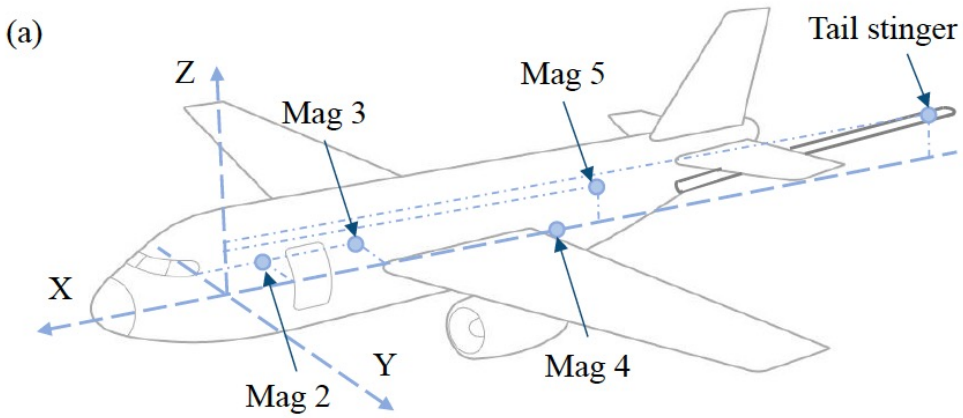

github.com/MIT-AI-Accelerator/MagNav.jl

Examples of results from TL calibration:

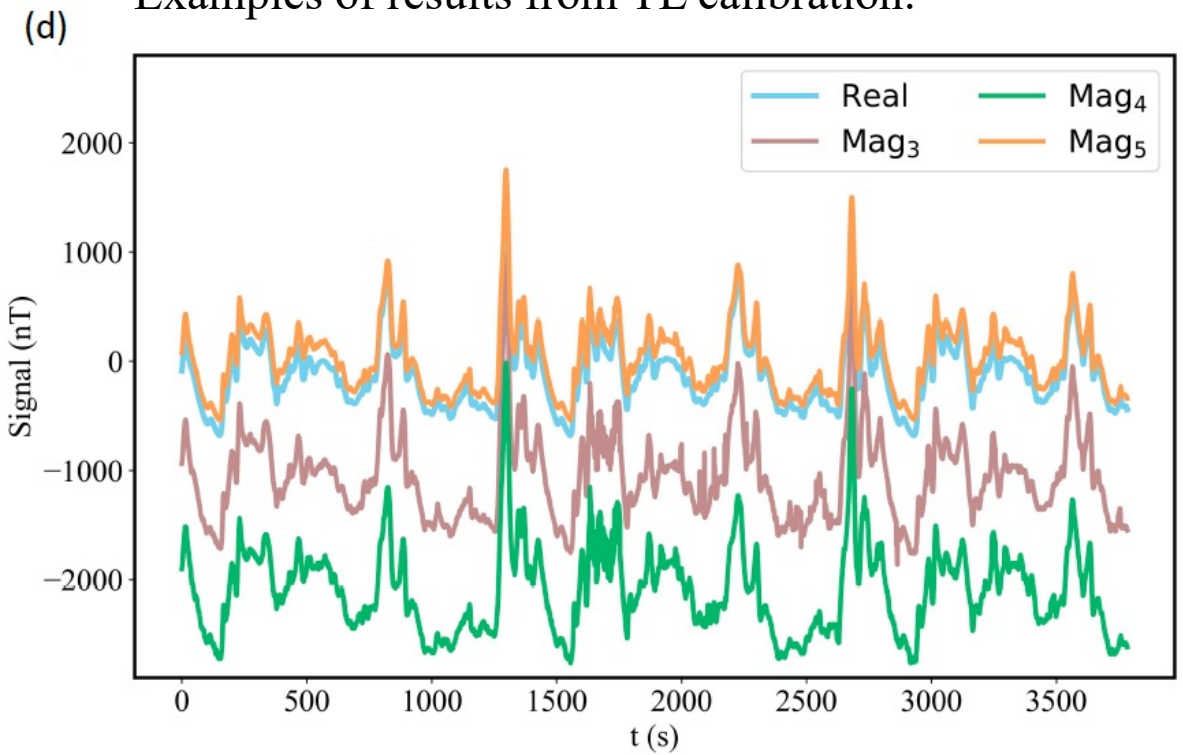

$$|\vec{B}_{\mathrm{e,\ TL}}| = |\vec{B}_{\mathrm{m}}| - B_{\mathrm{TL}}$$

Examples

TABLE II. Line number summary for flight 1003

Line number	Description	Training length (s)	Validation/Test length (s)
1003.02	Eastern Ontario Free-Fly 400m	2246.5	748.8
1003.03	Climb to 800m	61.3	20.4
1003.04	Eastern Ontario Free-Fly 800m	2877.7	959.2
1003.05	Transit at 800m	246.7	82.2
1003.06	Descend to 400m	83.5	27.8
1003.07	Transit to Renfrew Free-Fly	58.9	19.6
1003.08	Renfrew Free-Fly 400m	2581.9	860.6
1003.09	Climb to 800m	82.3	27.4

TABLE V. Line number summary for flight 1006

Line number	Description	Training length (s)	Validation/Test length (s)
1006.03	Climb to 17,000ft	448.3	149.4
1006.04	Compensation maneuvers at 17,000ft	2547.7	849.2
1006.05	Descent to 10,000ft	317.5	105.8
1006.06	Compensation maneuvers at 10,000ft	369.1	123.0
1006.07	Transit/Descent to Eastern Ontario	732.1	244.0
1006.08	Compensation maneuvers in Eastern Ontario at 400m	479.5	159.8

Additional Features Collected During Flight

61 other features recorded at the same time by some current and voltage sensors and readings from the INS system

Examples of some "most important" features:

TABLE I. Importance ranking of the features selected by a greedy algorithm

Features	Units	Description
flux_c_t	nT	Flux C: fluxgate total
cur_ac_lo	A	Current sensor: air conditioner fan low
ins_alt	m	INS computed elevation
flux_c_z	nT	Flux C: fluxgate z axis
flux_a_t	nT	Flux A: fluxgate total
vol_back_p	V	Voltage sensor: resolver board(+)
vol_back_n	V	Voltage sensor: resolver board(-)
ins_lat	rad	INS computed latitude
cur_com_1	A	Current sensor: aircraft radio 1
flux_c_y	nT	Flux C: fluxgate y axis
vol_acpwr	V	Voltage sensor: aircraft power
ins_wander	rad	INS computed wander angle
cur_flap	A	Current sensor: flap motor
vol_bat_2	A	Current sensor: battery 2
ins_roll	deg	INS computed aircraft roll

- Z.-M. Zhai, M. Moradi, L.-W. Kong, and Y.-C. Lai, "Detecting weak physical signal from noise: A machine-learning approach with applications to magnetic-anomaly guided navigation," *Physical Review Applied* **19**, 034030, 1-18 (2023).

Fluxgates B, C, D along x, y, and z axes have been used in TL calibration (Air Force – MIT MagNav Challenge)

Example of Estimated Earth's Magnetic Field Map in a Flying Region

$\vec{B}_{e,TL}$:

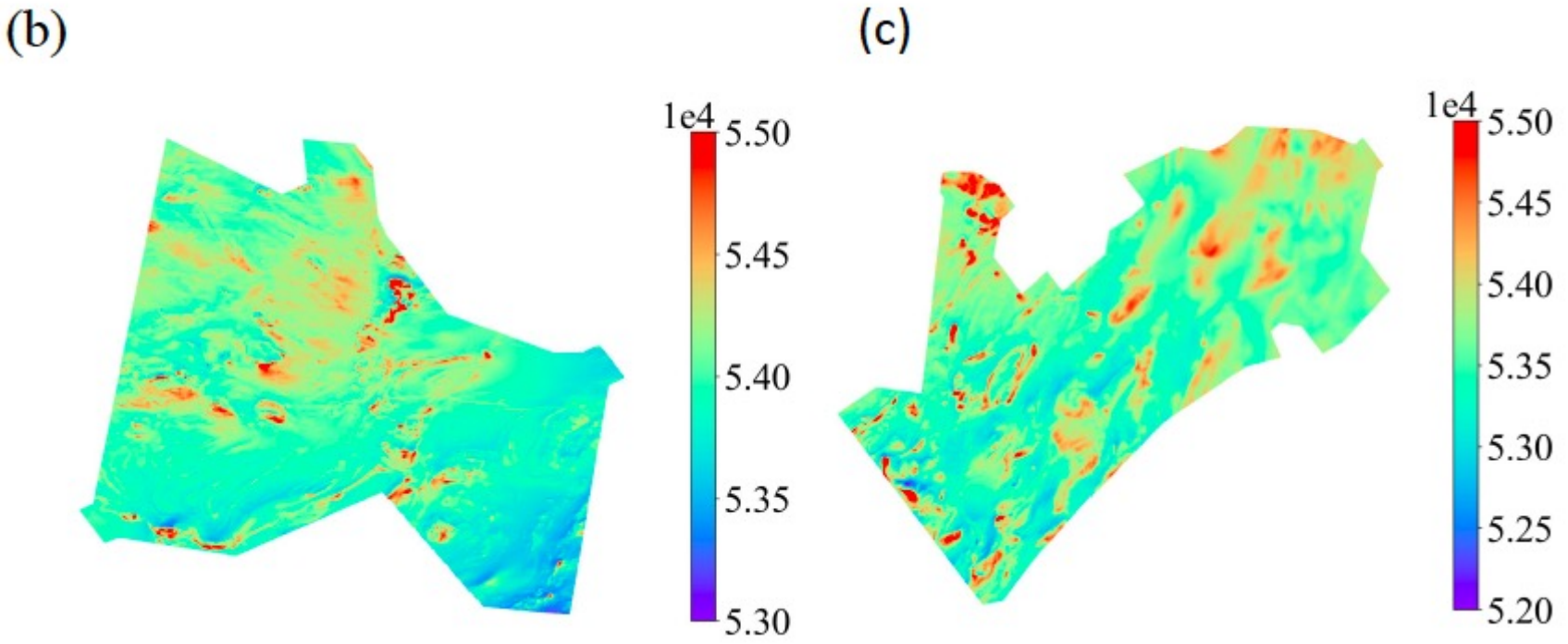

Units: nT

github.com/MIT-AI-Accelerator/MagNav.jl

Additional Features – How Many are Needed?

Determining the number of features as additional input signals (greedy algorithm)

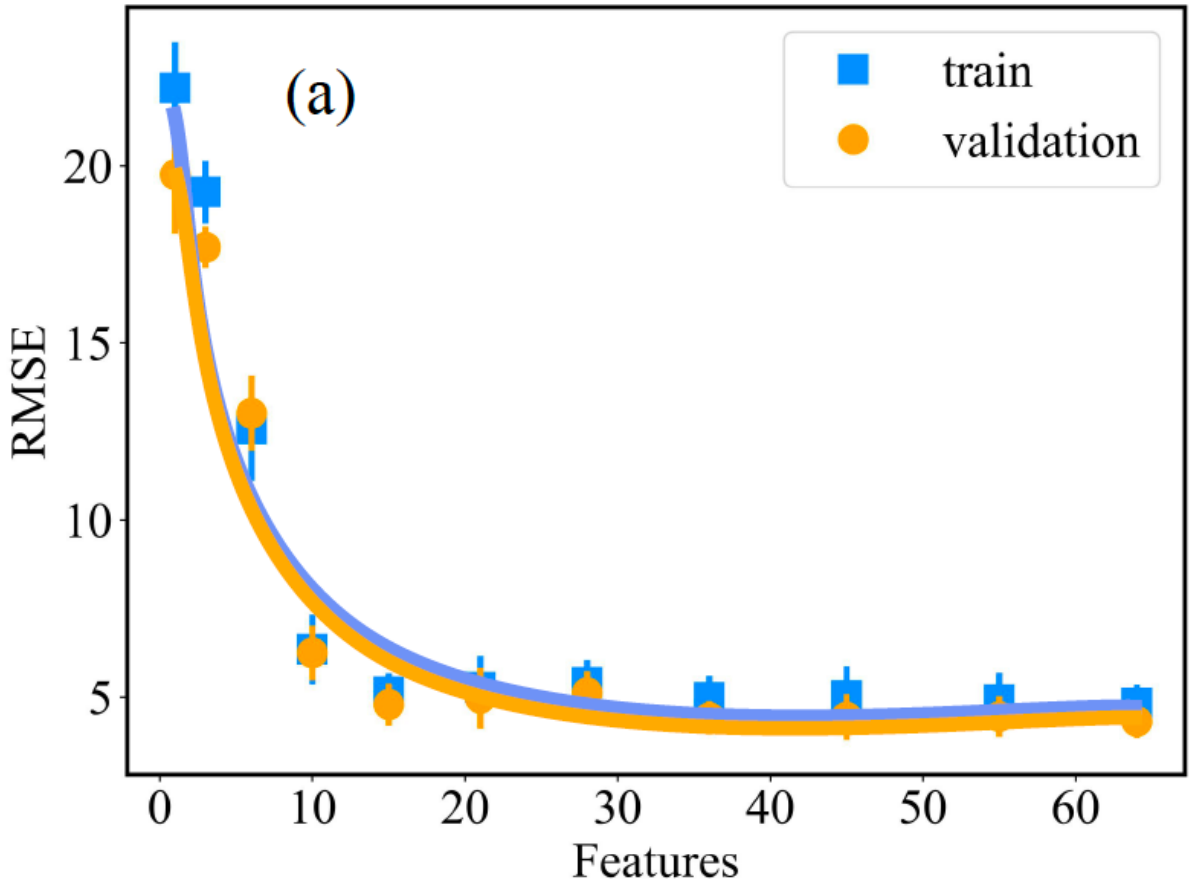

Machine Learning Scheme 1: Reservoir Computing

REPORT

Harnessing Nonlinearity: Predicting Chaotic Systems and Saving Energy in Wireless Communication

Herbert Jaeger*, Harald Haas
+ See all authors and affiliations

Science 02 Apr 2004:
Vol. 304, Issue 5667, pp. 78-80
DOI: 10.1126/science.1091277

PHYSICAL REVIEW LETTERS **120,** 024102 (2018)

Model-Free Prediction of Large Spatiotemporally Chaotic Systems from Data: A Reservoir Computing Approach

Jaideep Pathak,[1,2,*] Brian Hunt,[3,4] Michelle Girvan,[1,3,2] Zhixin Lu,[1,3] and Edward Ott[1,2,5]

PHYSICAL REVIEW RESEARCH **3**, 013090 (2021)

Machine learning prediction of critical transition and system collapse

Ling-Wei Kong,[1] Hua-Wei Fan,[2] Celso Grebogi,[3] and Ying-Cheng Lai[1,4,*]

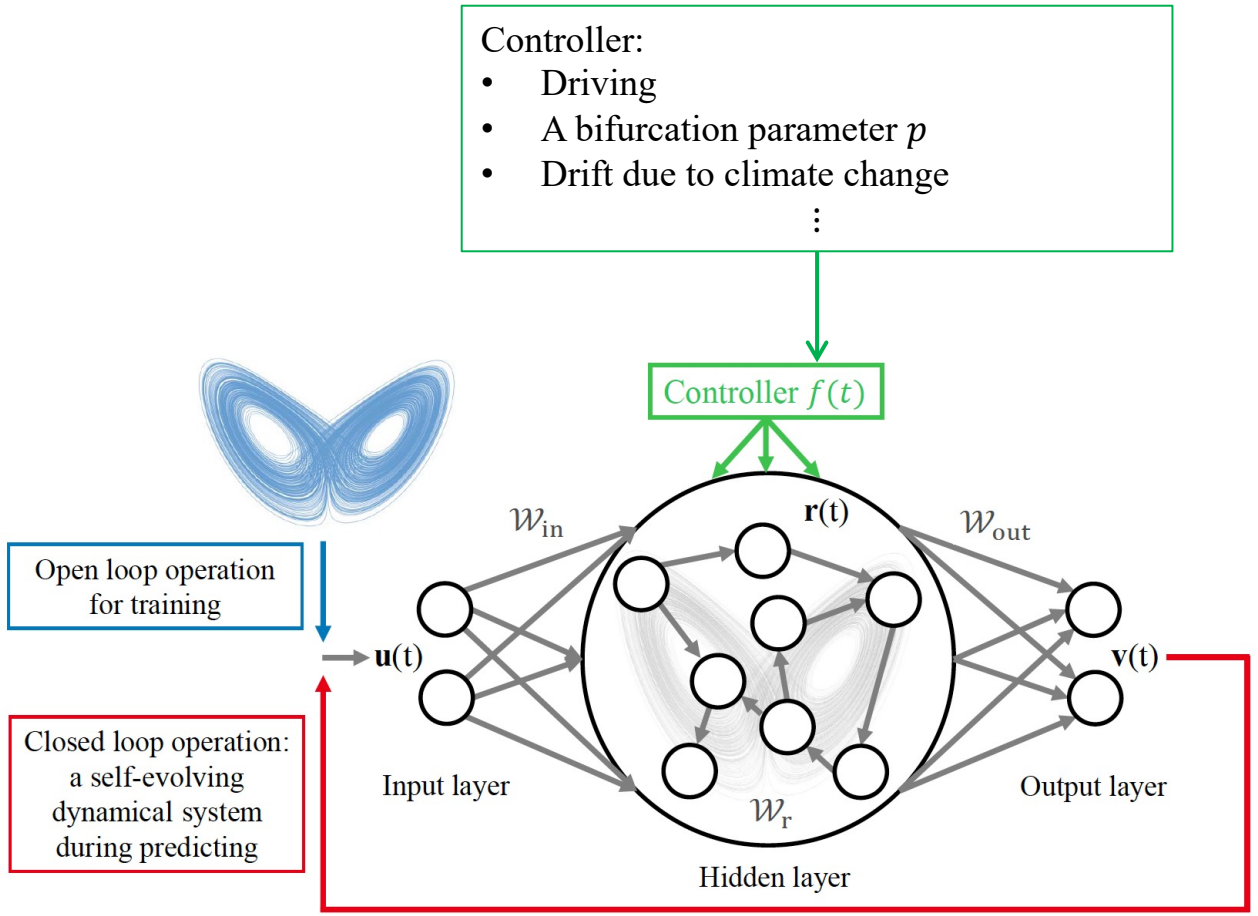

A digital twin for predicting the state evolution of nonlinear dynamical systems!

L.-W. Kong, Y. Weng, B. Glaz, M. Haile, and Y.-C. Lai, "Reservoir computing as digital twins of nonlinear dynamical systems," *Chaos* **33**, 033111, 1-21 (2023)

Reservoir Computing for Weak Signal Detection

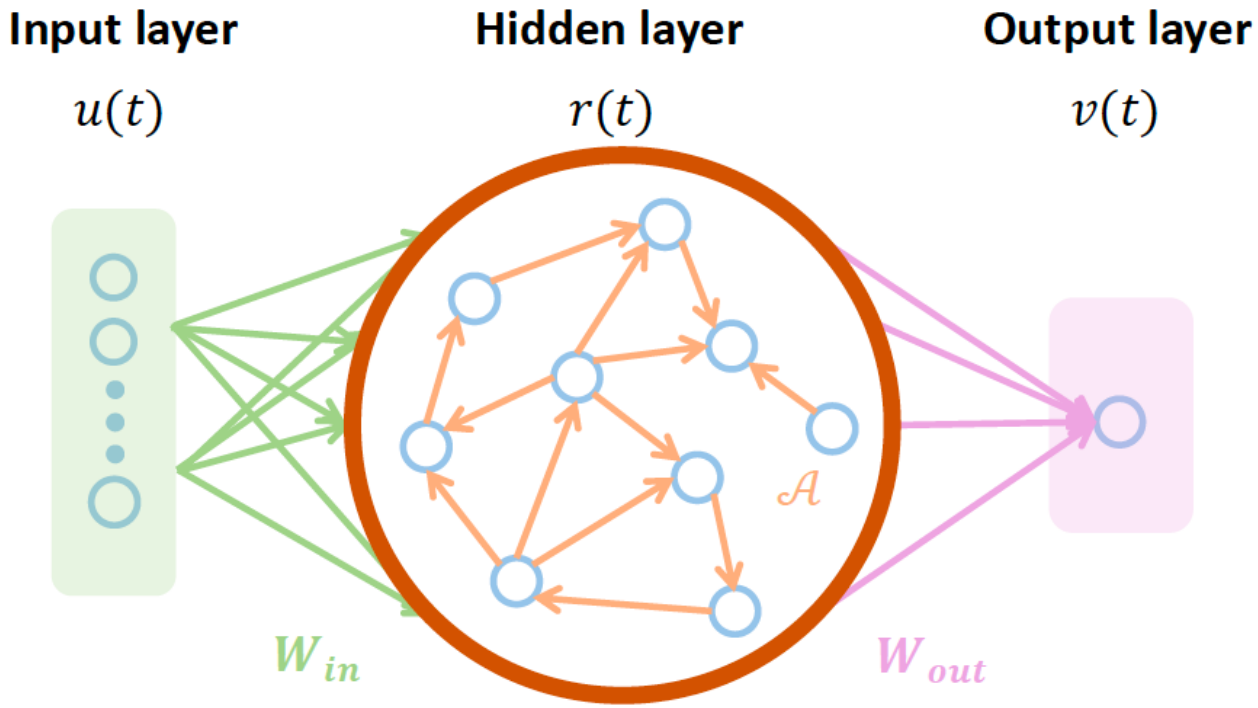

- Recurrent neural network architecture
- **Input signal is always available: a filtering problem**
- A large (usually complex) network in a single hidden layer

Z.-M. Zhai, M. Moradi, L.-W. Kong, and Y.-C. Lai, "Detecting weak physical signal from noise: A machine-learning approach with applications to magnetic-anomaly guided navigation," *Physical Review Applied* **19**, 034030, 1-18 (2023).

Reservoir Computing: Representative Results

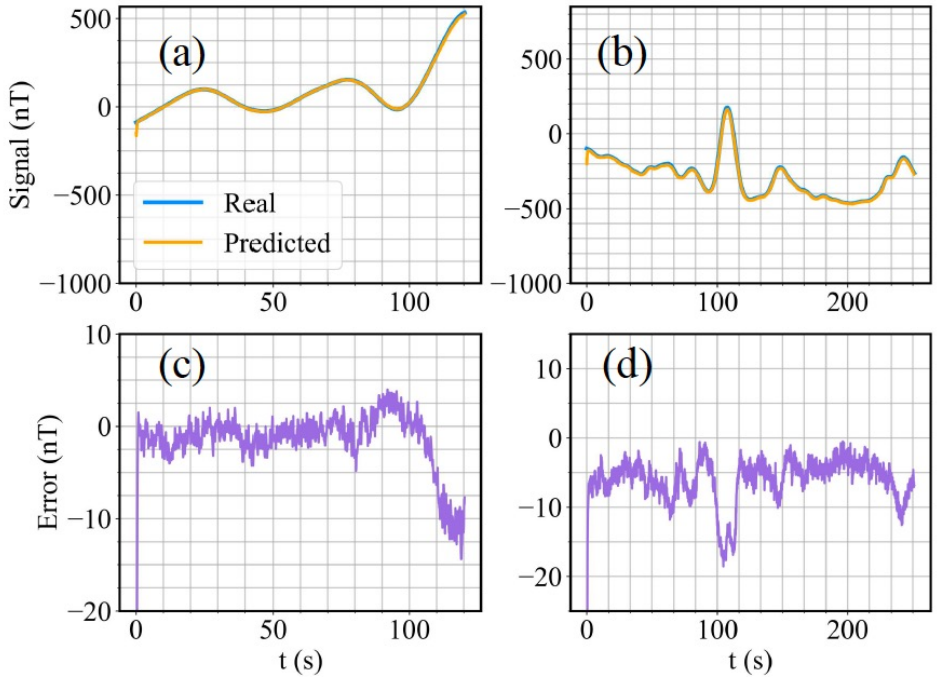

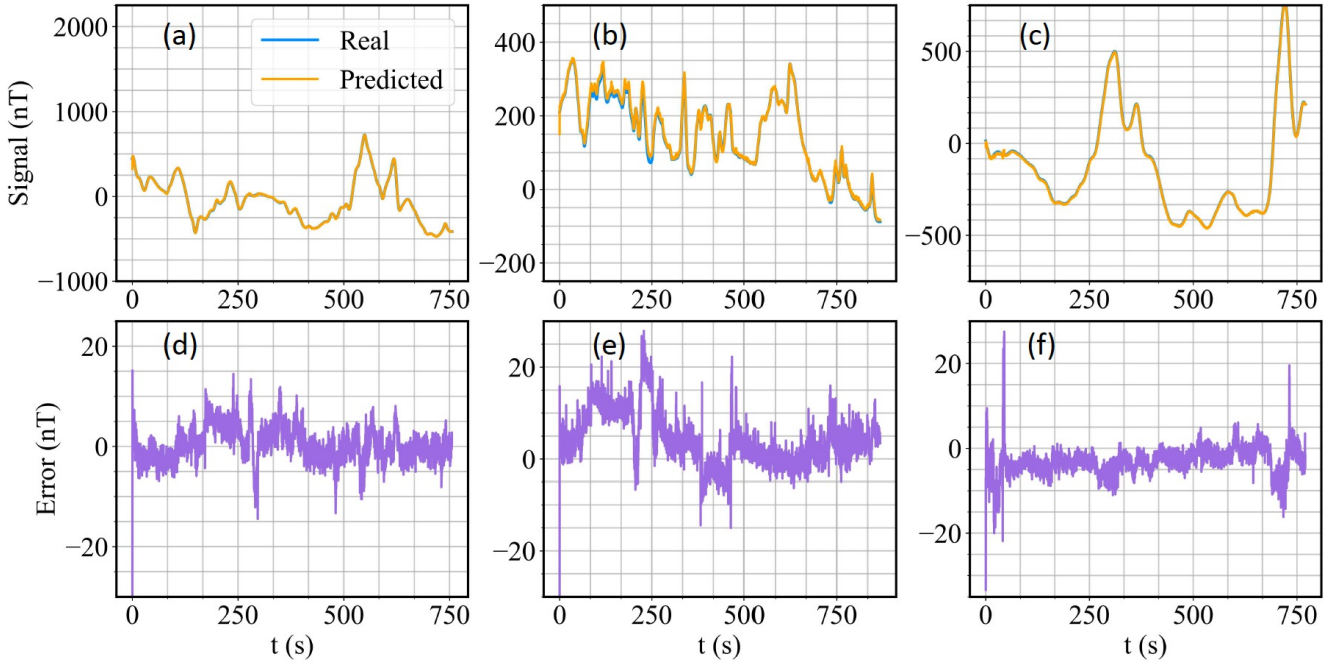

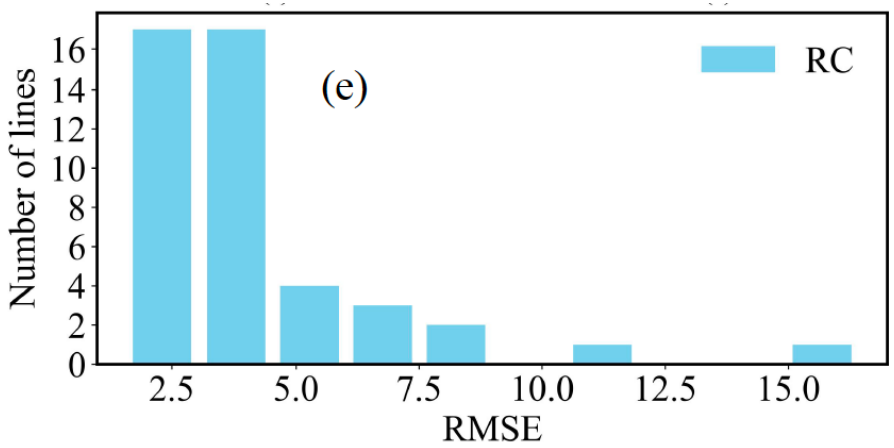

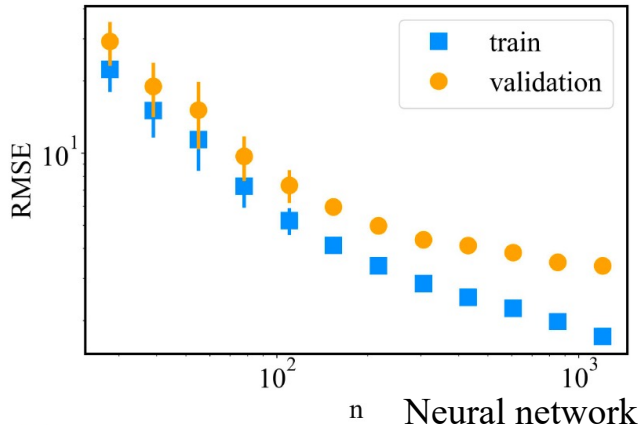

Machine-Learning Scheme 2: Time-Delayed Feed Forward Neural Networks

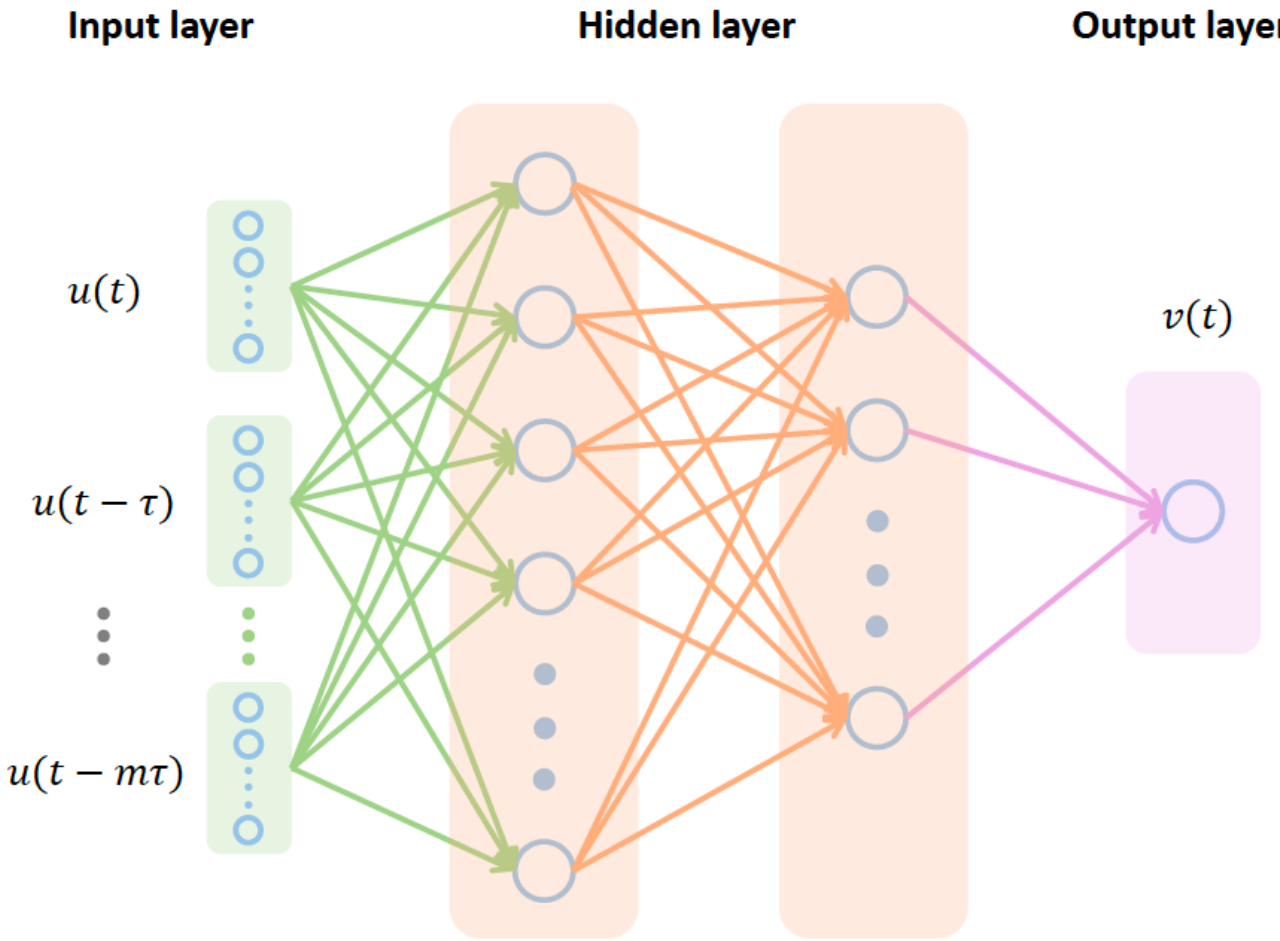

- A few hidden layers, each with a small neural network
- Memory property realized by delay-coordinate embedding
- High computational efficiency

ARTICLE
https://doi.org/10.1038/s41467-021-25801-2 OPEN

Next generation reservoir computing

Daniel J. Gauthier[1,2✉], Erik Bollt[3,4], Aaron Griffith[1] & Wendson A. S. Barbosa[1]

NATURE COMMUNICATIONS | (2021)12:5564 | https://doi.org/10.1038/s41467-021-25801-2

Time Delayed Feed Forward Neural Networks

Determining the embedding dimension

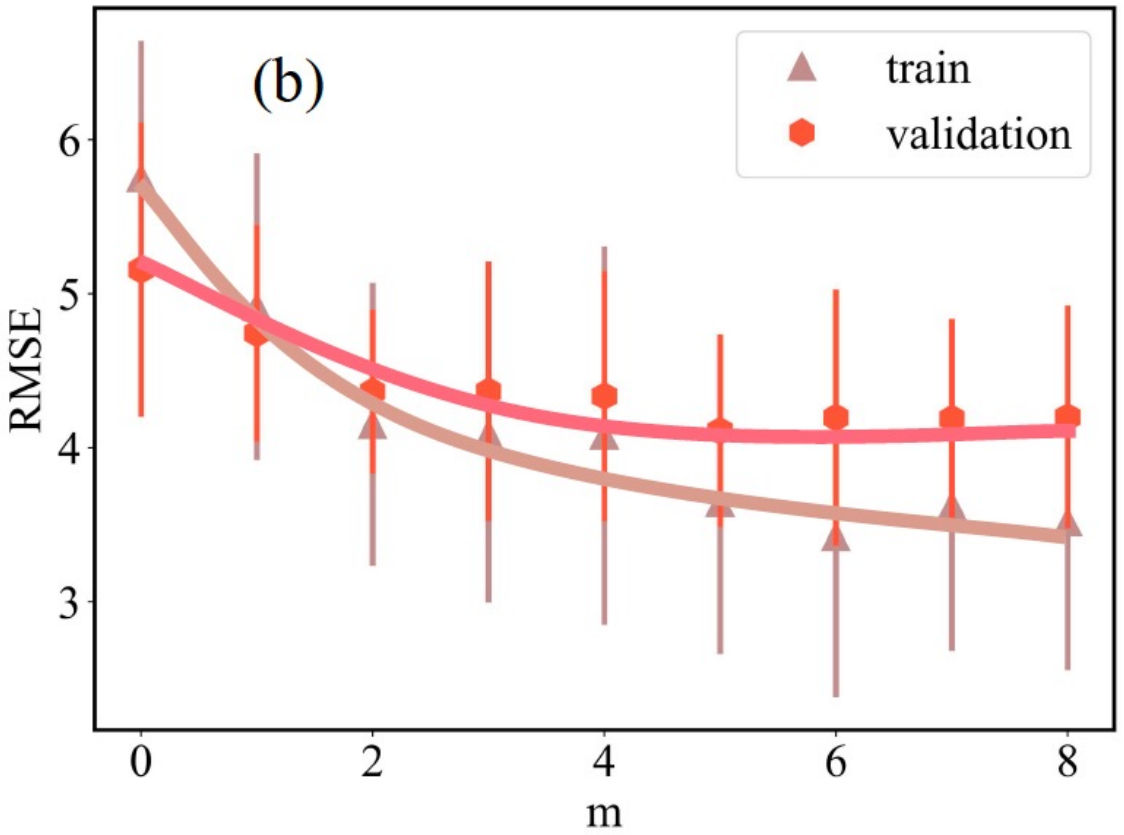

Results from Time-Delayed Feed Forward Neural Networks

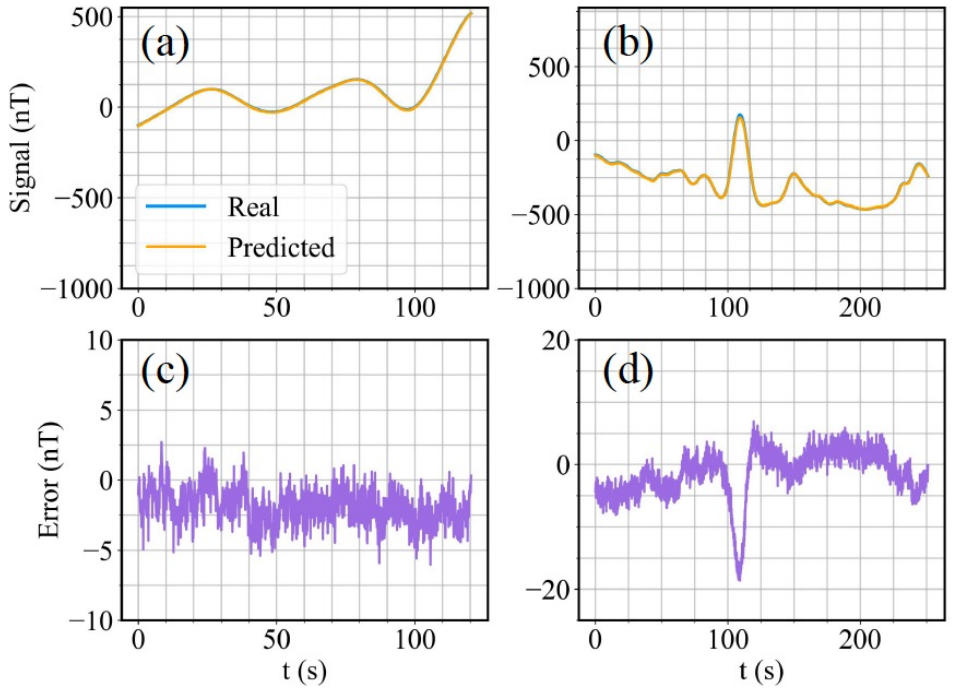

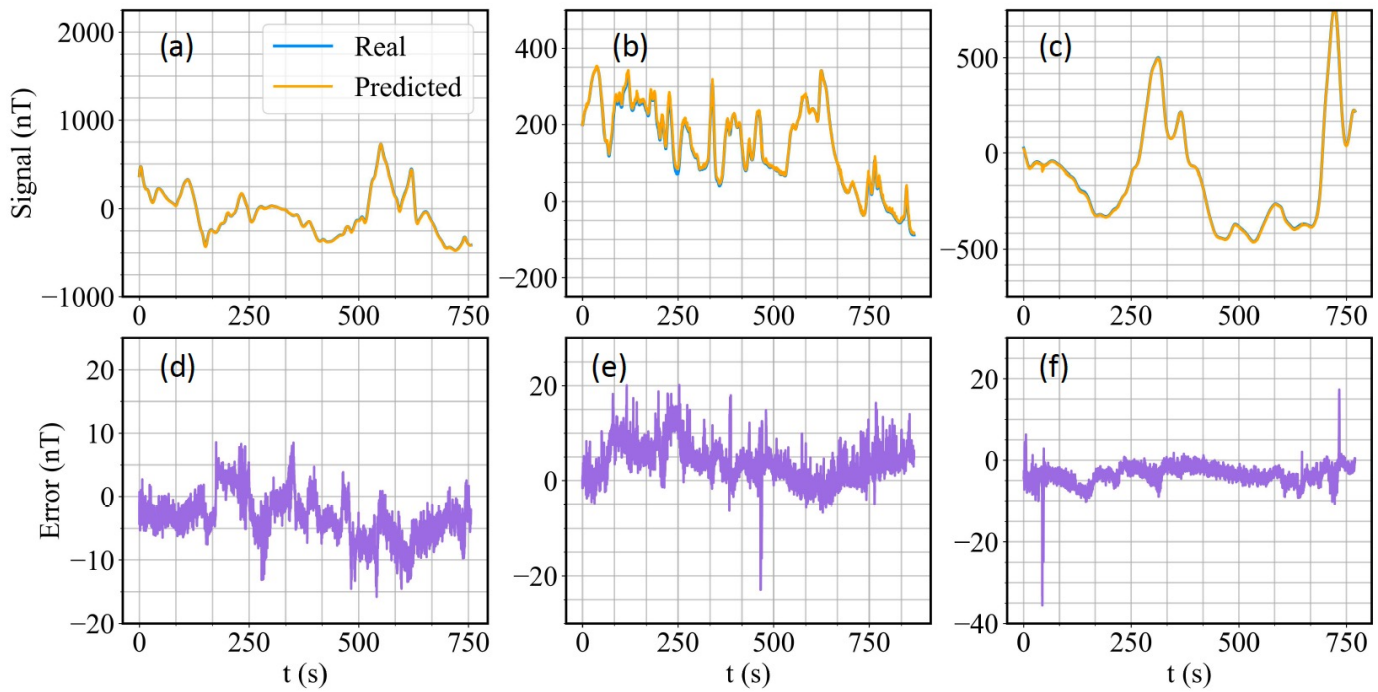

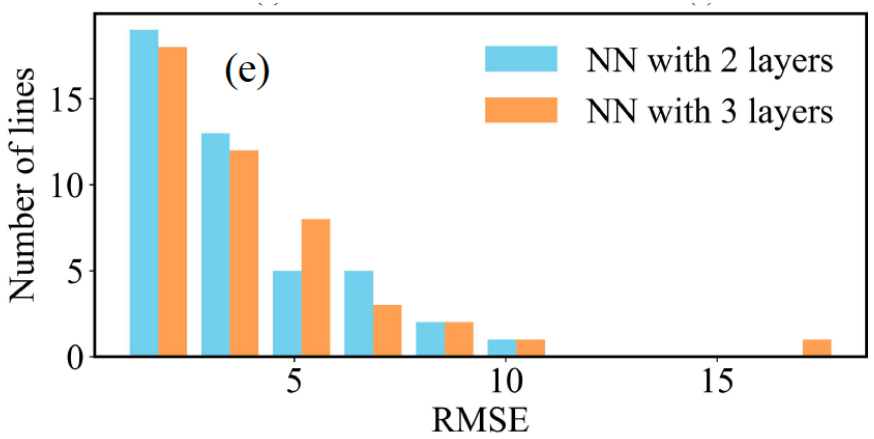

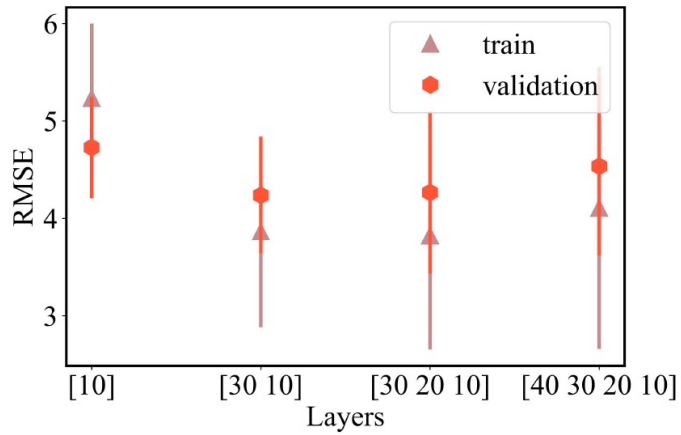

An Alternative Machine-Learning Approach

A Decision Tree

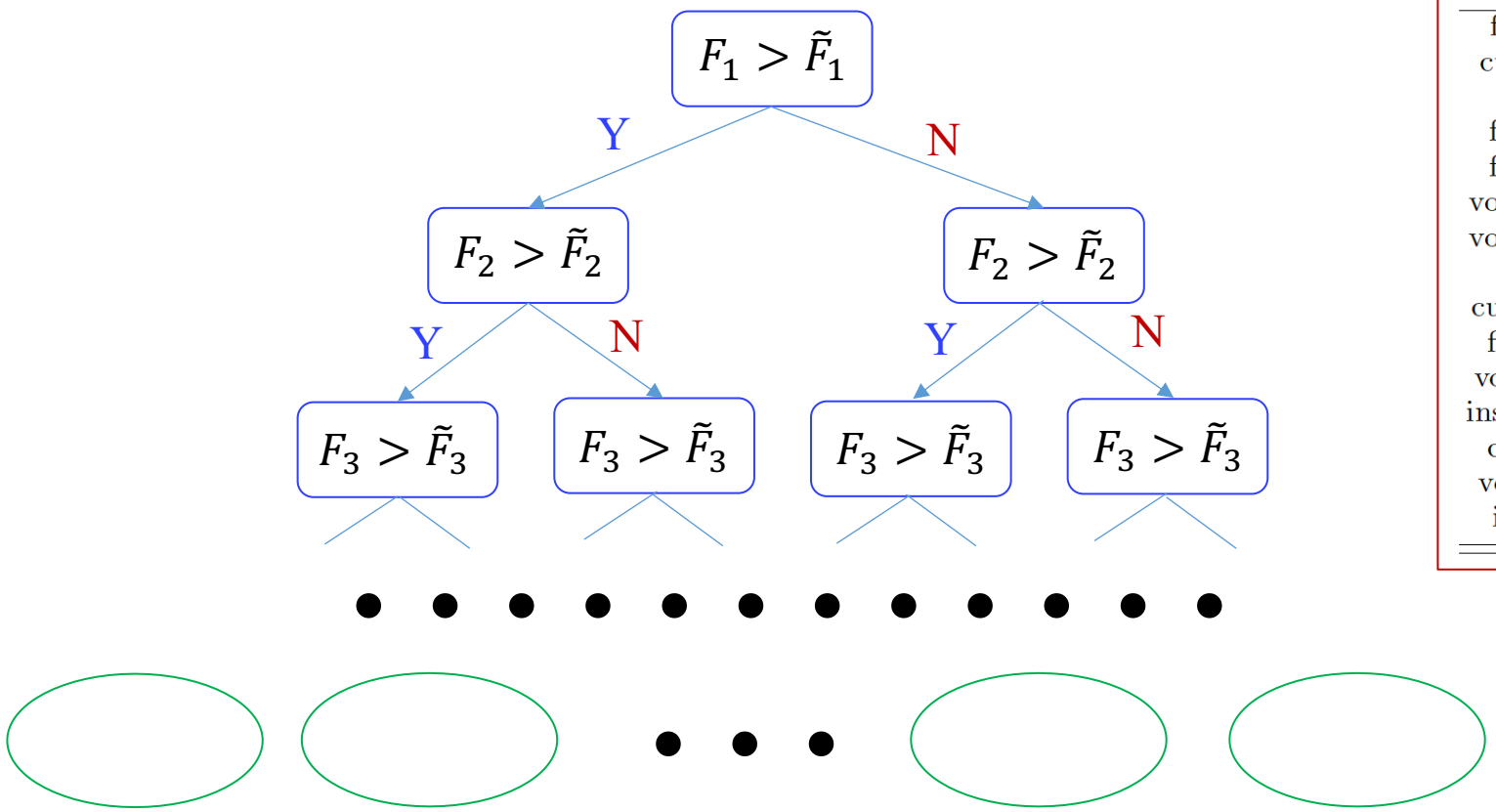

Example of features:

TABLE I. Importance ranking of the features selected by a greedy algorithm

Features	Units	Description
flux_c_t	nT	Flux C: fluxgate total
cur_ac_lo	A	Current sensor: air conditioner fan low
ins_alt	m	INS computed elevation
flux_c_z	nT	Flux C: fluxgate z axis
flux_a_t	nT	Flux A: fluxgate total
vol_back_p	V	Voltage sensor: resolver board(+)
vol_back_n	V	Voltage sensor: resolver board(-)
ins_lat	rad	INS computed latitude
cur_com_1	A	Current sensor: aircraft radio 1
flux_c_y	nT	Flux C: fluxgate y axis
vol_acpwr	V	Voltage sensor: aircraft power
ins_wander	rad	INS computed wander angle
cur_flap	A	Current sensor: flap motor
vol_bat_2	A	Current sensor: battery 2
ins_roll	deg	INS computed aircraft roll

Parameters to be trained:
$\tilde{F}_1, \tilde{F}_2, \tilde{F}_3, \ldots$

Labels: a large collection of possible values of the weak signal (to be detected) in a suitable range (values in the training set + random values)

Random Forest

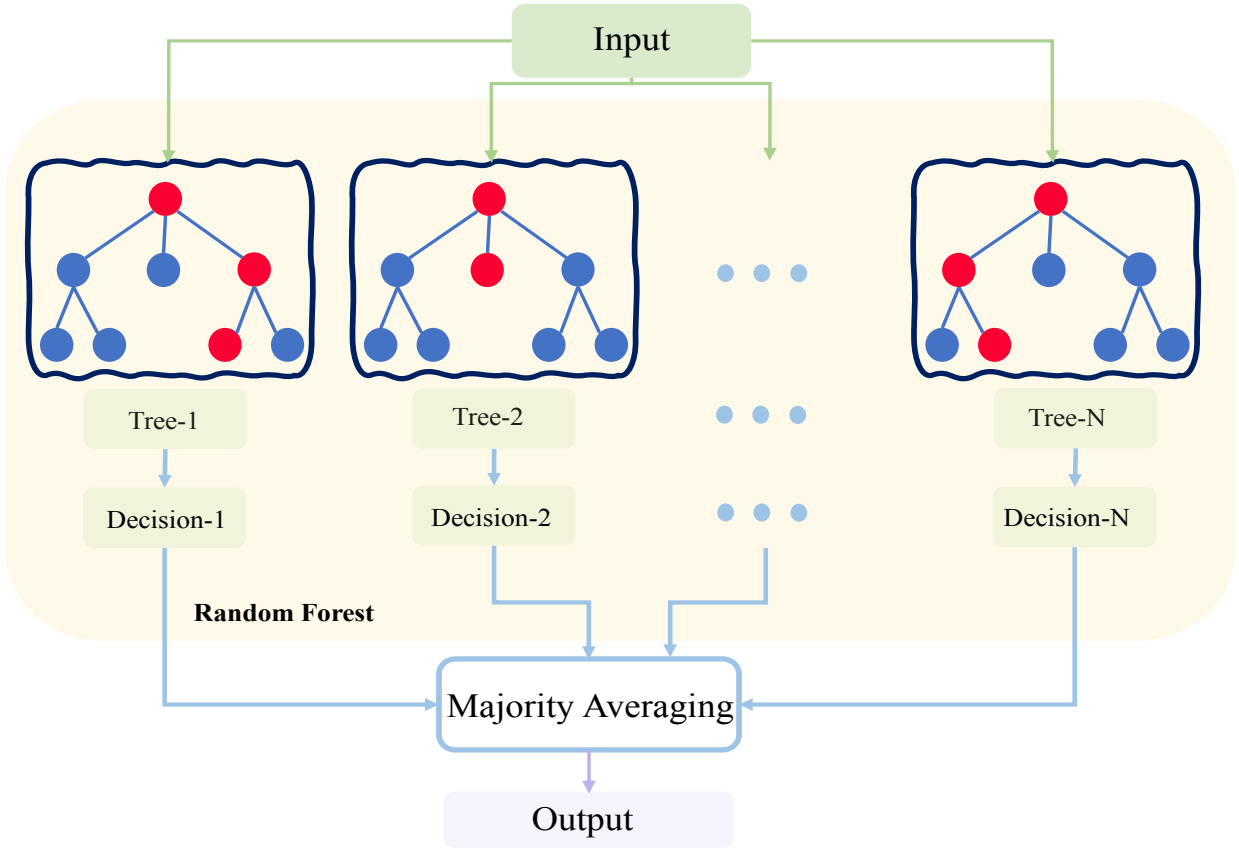

Random Forest:

- An ensemble of decision trees;
- Each tree is trained using a different subset of data

Training:

- Training a tree with a randomly selected set of features and a fraction of the available training data;
- Adding the trained tree to the "Forest"
- Adding more trained trees to the "Forest"

Prediction:

- Combining all predictions from the trees in the "Forest"

A. Moradi, Z.-M. Zhai, A. Nielsen, and Y.-C. Lai, "Random forest for accurate detection of weak physical signals," working paper (2023)

Parameter Tracking

A chaotic food-chain

$$\frac{dR}{dt} = R(1 - \frac{R}{K}) - \frac{x_c y_c CR}{R + R_0},$$

$$\frac{dC}{dt} = x_c C(\frac{y_c R}{R + R_0} - 1) - \frac{x_p y_p PC}{C + C_0},$$

$$\frac{dP}{dt} = x_p P(\frac{y_p C}{C + C_0} - 1),$$

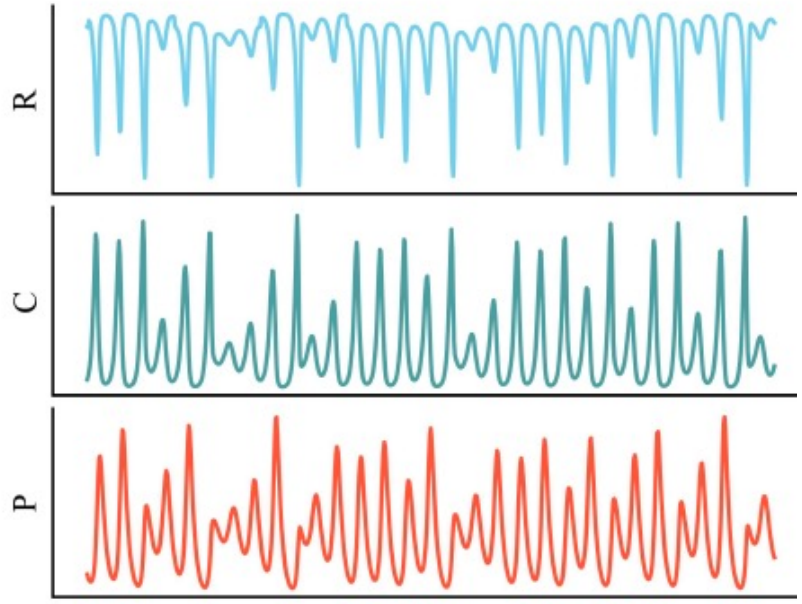

$K = ?$ or $K(t) = ?$

Inverse Problem

Ongoing Work: Machine Learning with Partial Measurements

Full state of the system

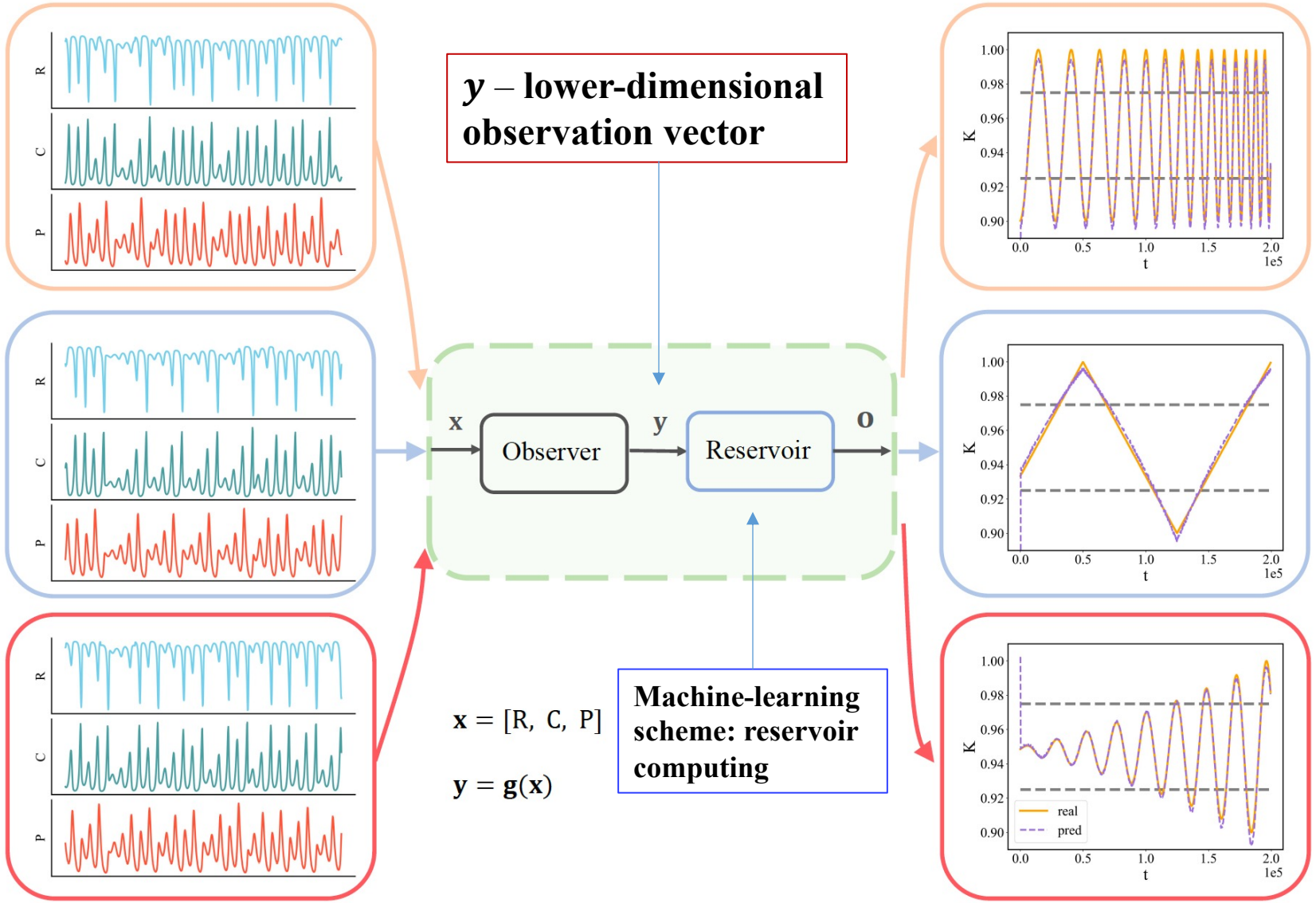

Parameter as a function of time

Zheng-Meng Zhai, Mohammadamin Moradi, Bryan Glaz, Mulugeta Haile, and Ying-Cheng Lai, "Tracking parameter variations in nonlinear dynamical systems using machine learning," preprint (2023)

Machine-Learning Strategy - Training

Assumption:
Observations from a small number of distinct parameter values can be collected in a well-controlled, laboratory environment

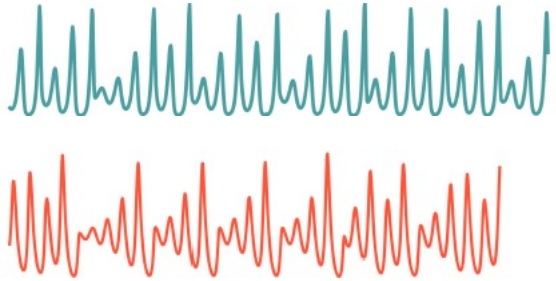

Parameter value K_1

Parameter value K_2

Training
- Laboratory calibration

Machine-learning input

Learning goal

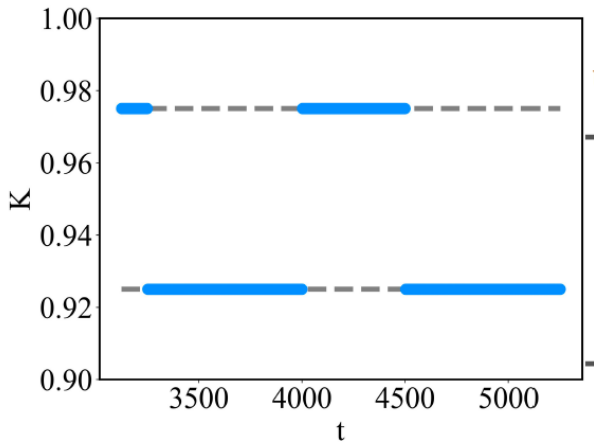

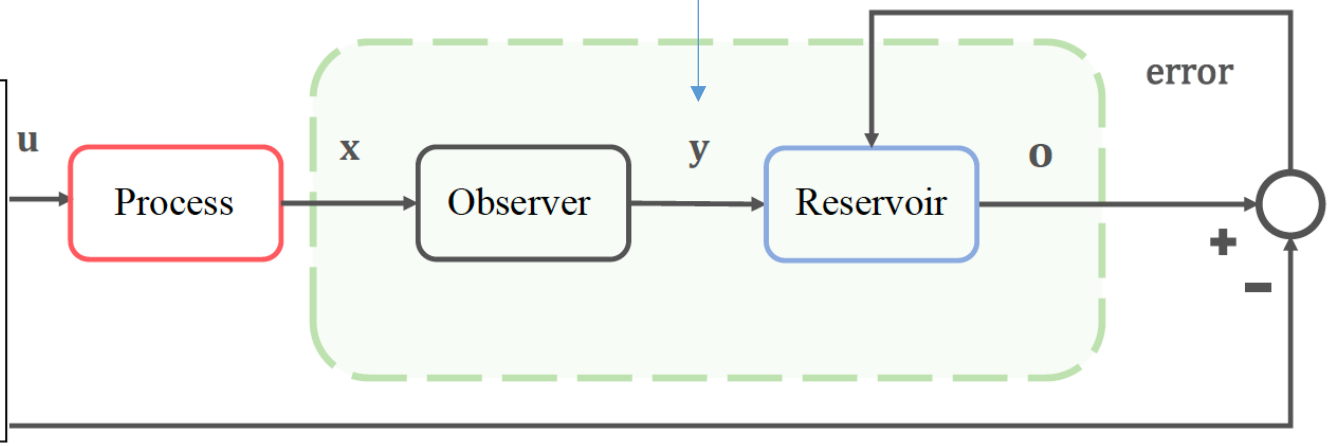

Machine-Learning Strategy: Testing or Deployment

During testing or deployment:

- Parameters are no longer accessible
- Their variations are unknown
- Partial state observations are available – machine-learning inputs

Machine-learning output: **Time variations of the parameter**

Reservoir computing

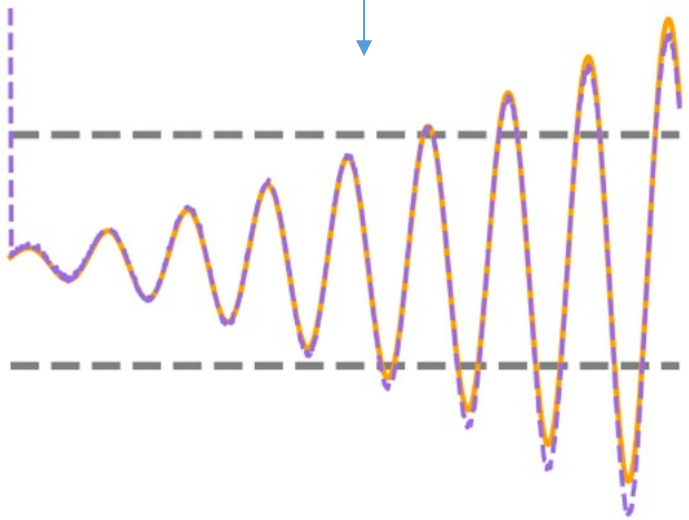

Machine-learning input

Machine-learning scheme: Adaptable Reservoir Computing – Why?

Conclusion

- The relation between the error in the detected earth's anomaly magnetic field and positioning precision is nonlinear.
- An error below 6.5 nT corresponds to the positioning error of less than 45 m.
- Empirically, the position error is approximately about 10 - 40 m when the magnetic signa error is around 4 nT.
- The mean magnetic signal errors from both reservoir computing and time-delayed feed forward neural networks is about 4 nT
- The anomaly field detected by reservoir computing and feedforward neural networks can be used for actual aircraft navigation positioning.
- Alternative machine-learning method: Random Forest

Ongoing work:

Developing **Transfer Learning** methods to deal with the situations where tail stinger measurements are not available - collaboration with Dr. Aaron Nielsen from Air Force Institute of Technology

K = Constant: Parameter Identification

- **Least squares fitting** – e.g., E. W. Weisstein, Least squares fitting, https://mathworld.wolfram.com/ (2002)
- **Maximum likelihood estimation** – e.g., J.-X. Pan and K.-T. Fang, Maximum likelihood estimation, pp. 77-158 in Growth Curve Models and Statistical Diagnostics (Springer, 2002)
- **Bayesian estimation** – e.g., A. J. Haug, Bayesian Estimation and Tracking: A Practical Guide (John Wiley & Sons, 2012)
- **Genetic algorithm** – e.g., L. Yao and W. A. Sethares, Nonlinear parameter estimation via the genetic algorithm, IEEE Trans. Signal Proc. **42**, 927 (1994)
- **Neural networks** – e.g., P. Guo, M. R. Lyu, and C. L. P. Chen, Regularization parameter estimation for feedforward neural networks, IEEE Trans. Sys. Man Cyber. B **33**, 35 (2003)
- **Markov chain Monte Carlo** – e.g., F. Yandun, M. Torres-Torriti, and F. Auat Cheein, Markov chain Monte Carlo parameter estimation for nonzero slip models of wheeled mobile robots: A skid steer case study, J. Mech. Robot. **13** (2021)
- **Kalman filter** – e.g., G. Evensen, The ensemble Kalman filter for combined state and parameter estimation, IEEE Cont. Sys. Mag. **29**, 83 (2009); L. Ljung, Asymptotic behavior of the extended Kalman filter as a parameter estimator for linear systems, IEEE Trans. Auto. Cont. **24**, 36 (1979).

Time-Varying Parameter K(t): Parameter Tracking

Machine-learning methods:

- Y. Chen and Y. Zhou, Machine learning based decision making for time varying systems: Parameter estimation and performance optimization, Knowledge-Based Sys. **190**, 105479 (2020).
- Y. Zhang, Neural network algorithm with reinforcement learning for parameters extraction of photovoltaic models, IEEE Trans. Neural Net. Learning Sys. (2021).
- A. B. Abdusalomov, F. Safarov, M. Rakhimov, B. Turaev, and T. K. Whangbo, Improved feature parameter extraction from speech signals using machine learning algorithm, Sensors **22**, 8122 (2022).
- J. Hannink, T. Kautz, C. F. Pasluosta, K.-G. Gabmann, J. Klucken, and B. M. Eskofier, Sensor-based gait parameter extraction with deep convolutional neural networks, IEEE J. Biomed. Health Info. **21**, 85 (2016).
- X. Chen, Y. Tian, T. Zhang, and J. Gao, Differential evolution based manifold gaussian process machine learning for microwave filter's parameter extraction, IEEE Access **8**, 146450 (2020).
- M.-Y. Kao, F. Chavez, S. Khandelwal, and C. Hu, Deep learning-based BSIM-CMG parameter extraction for 10-nm finfet, IEEE Trans. Elec. Dev. **69**, 4765 (2022).

Limitation: full-state measurements – time series of all dynamical variables of the system are required